DOI: 10.24850/j-tyca-13-06-02

Articles

Experimental study and dynamic simulation of the adsorption of Cd+2 and Pb+2 using the cocoa shell in a fixed-bed column

Estudio experimental y simulación dinámica de la adsorción de Cd^{+2} y Pb^{+2} utilizando cáscara de cacao en columna de lecho fijo

Mayra Vera[1], ORCID: https://orcid.org/0000-0002-0240-9147

Sonia Astudillo[2], ORCID: https://orcid.org/0000-0002-4646-1959

Diego M. Juela[3], ORCID: https://orcid.org/0000-0002-3398-2069

[1]School of Chemical Engineering, School of Chemical Sciences, Universidad de Cuenca, Cuenca, Ecuador, mayra.vera@ucuenca.edu.ec

[2]Center for Environmental Studies, Department of Applied Chemistry and Production Systems, Faculty of Chemical Sciences, Universidad de Cuenca, Cuenca, Ecuador, sonia.astudilloo@ucuenca.edu.ec

[3]Center for Environmental Studies, Department of Applied Chemistry and Production Systems, Faculty of Chemical Sciences, Universidad de Cuenca, Cuenca, Ecuador, diego.juela@ucuenca.edu.ec

Corresponding author: Mayra Vera, mayra.vera@ucuenca.edu.ec

Abstract

Using biomass as an adsorbent constitutes a potential alternative for removing heavy metals in industrial wastewater, representing a high environmental risk. In this work, the adsorption of Pb^{+2} and Cd^{+2} was performed using the cocoa shell as an adsorbent in columns, and the dynamic simulation of the process using the Aspen Adsorption® V10 software, to validate the simulation results and those obtained experimentally. The simulator and experimental rupture curves converge in almost the entire trajectory, with slight variations in the final stretch of the curve, with the rupture times coinciding for both metals, giving correlation coefficients (R^2) of 0.984 and 0.998 for Pb^{+2} and $Cd^{+2,}$ respectively, as well as error values (SSE) less than 5 %. The effect produced by the variation of the bed height and the flow rate in the rupture curves was analyzed; as the bed height increases and the flow rate decreases, the rupture time increases, favoring the adsorption of both metals. The results of this research show the importance of the use of Aspen Adsorption® software in the biosorption process due to the similarity with experimental results, providing its use saving time and resources.

Keywords: Cocoa shell, biosorption, heavy metals, Aspen Adsorption®, simulation.

Tecnología y Ciencias del Agua

OPEN ACCESS

Check for updates

Resumen

El uso de biomasa como adsorbente constituye una alternativa potencial para la remoción de metales pesados presentes en aguas residuales industriales, lo cual representa un alto riesgo para el medio ambiente. En este trabajo se realizó la adsorción de Pb^{+2} y Cd^{+2} utilizando la cáscara de cacao como adsorbente en columnas y la simulación dinámica del proceso utilizando el *software* Aspen Adsorption® V10, con la finalidad de validar los resultados de la simulación y los obtenidos experimentalmente. Las curvas de ruptura del simulador y las experimentales convergen en casi toda la trayectoria, existiendo ligeras variaciones en el tramo final de la curva, coincidiendo los tiempos de ruptura para ambos metales, dando coeficientes de correlación (R^2) de 0.984 y 0.998 para el Pb^{+2} y Cd^{+2}, respectivamente, así como valores de error (SSE) inferiores al 5 %. Se analizó el efecto que produce la variación de la altura del lecho y el caudal en las curvas de ruptura; a medida que aumenta la altura del lecho y disminuye el caudal aumenta el tiempo de ruptura, favoreciendo la adsorción de ambos metales. Los resultados de esta investigación muestran la importancia del uso del *software* Aspen Adsorption® en el proceso de biosorción debido a la similitud con resultados experimentales, proporcionando su uso un ahorro de tiempo y recursos.

Palabras clave: cáscara de cacao, biosorción, metales pesados, Aspen Adsorption®, simulación.

Received: 06/24/2020

Accepted: 08/15/2021

Introduction

Heavy metals in wastewater are present due to human and natural factors (Sörme & Lagerkvist, 2002). Volcanic activities and soil erosion constitute the natural sources. In contrast, effluents from mining and extraction, textile activities, metal finishing and electroplating operations, industrial nuclear energy, domestic sewage, and agricultural runoff make up anthropogenic activities (Musilova, Arvay, Vollmannova, Toth, & Tomas, 2016; Akpor, Ohiobor, & Olaolu, 2014). The release of these wastewaters without treatment is the main source of heavy metal contamination in aquatic ecosystems; their presence in fresh and marine water bodies constitutes a real threat to all living organisms, even at low concentrations (Akif *et al*., 2002). Lead (Pb^{2+}) and cadmium (Cd2+) are two of the metals with the highest degree of toxicity (Rana, Tangpong, & Rahman, 2018); Their ability to bioaccumulate in animals and plants endangers the human food chain. Recent studies in several countries have reported the

bioaccumulation of Cd2+ and Pb^{2+} in freshwater and marine fish (Khanipour, Ahmadi, & Seifzadeh, 2018); similarly, Cd2+ has bioaccumulated in rice plantations (Besante, Niforatos, & Mousavi, 2011; Kong *et al*., 2018). Even in countries such as Australia, China, Saudi Arabia, India, Nigeria, Pakistan, Ethiopia, the Slovak Republic, Kenya, and Germany, toxic levels of Cd2+ and Pb^{2+} have been detected in vegetables, fruits, cereals, legumes, and nuts, related to the use of contaminated irrigation water (Yadav, Yadav, & Shukla, 2013; Khan, Ahmad, Ashraf, & Parveen, 2015). In this way, these metals easily enter the human food chain, producing carcinogenic effects and serious health problems.

Due to the foregoing, the search for technologies for the removal of heavy metals from industrial effluents is of utmost importance. Among the technologies that have been used for the treatment of wastewater containing heavy metals, there is membrane filtration (Schwarze *et al*., 2015; Gherasim & Mikulášek, 2014); ion exchange (Cegłowski & Schroeder, 2015; Jokar, Mirghaffari, Soleimani, & AJabbari, 2019); adsorption with activated carbon and carbon nanotubes (Kończyk, Żarska, & Ciesielski, 2019); chemical precipitation ((Byambaa, Dolgor, Shiomori, & Suzuki, 2018; Guo *et al*., 2015); electrocoagulation (Ferniza-García, Amaya-Chávez, Roa-Morales, & Barrera-Díaz, 2017; Khosa *et al*., 2013); coagulation and flocculation, electrocoagulation, flotation ((Mohammed, Ebrahim, & Alwared 2013; Taseidifar, Makavipour, Pashley, & Mokhlesur-Rahman, 2017), and photocatalysis (Mohammed *et al*., 2013; Taseidifar *et al*., 2017). All these technologies have technical and economic

constraints; some are expensive for large volumes of effluent or inefficient at low concentrations, producing large amounts of sludge and toxic products. Due to this, in recent decades, novel, economic and efficient technologies such as phytoremediation, biosorption, and the use of polymers and biopolymers have been developed.

Biosorption is a pollutant removal process (adsorbate) using biological materials (biosorbents) such as bacteria and algae (living biomass), as well as natural agricultural and industrial materials (dead biomass). Concerning the latter, in the literature, there are multiple studies where sugarcane bagasse, peach and apricot seeds, cabbage and cauliflower residues, wood, cocoa husk, barley straws, Neem bark, palm kernels, wheat straw, cassava shell, mussel shell, pinus ashes, oak ash, pinus bark, and hemp residues have been used as biosorbents for the removal of Cd2+ and Pb^{2+}, reaching removal percentages above 90 % (He *et al*., 2017; Li, Zhang, Li, Wang, & Ali, 2016; Mohamed, Ahmed, Tantawy, Gomaa, & Mahmoud, 2016). Experimental biosorption studies can be carried out in batch or continuous mode. The approach of the studies in discontinuous or batch mode is to determine the adjustment of the adsorbate-adsorbent system to an equilibrium model (Isotherms) (He *et al*., 2017; Li *et al*., 2016; Mohamed *et al*., 2016), while the studies in fixed-bed columns seek to fit the experimental results to mathematical models that describe the dynamic behavior of biosorption. Experimentation, whether in continuous or discontinuous mode, requires financial resources and time. In recent years, several researchers have

chosen to use advanced software to simulate the biosorption process (He *et al*., 2017; Li *et al*., 2016; Mohamed *et al*., 2016).

Aspen Adsorption® is a complete flow diagram simulator for the design, simulation, and optimization of industrial gas and liquid adsorption processes (He *et al*., 2017; Li *et al*., 2016; Mohamed *et al*., 2016). This software allows the researcher to save time and operating costs and determine the performance of biosorbents without experimentation. In the literature consulted, few studies use Aspen Adsorption to simulate the removal of heavy metals. Most of these studies do not compare the results obtained in the simulator with experimental data.

The main objective of this research was to compare the adsorption of Cd2+ and Pb^{2+} into cocoa shells and simulate the breakthrough curves using Aspen Adsorption®, as well as to evaluate the effect on the breakthrough curves when varying the flow rate and bed height.

Materials and methods

Preparation of biosorbent and solutions

The cocoa shell waste was collected from the farms of Portovelo, a coastal area in southern Ecuador. The samples were subjected to a treatment that consisted of multiple washing with distilled water, drying in the sun for ten days, a subsequent crushing with a hammer mill, and finally, size classification using a No.18 sieve, obtaining a coarse fraction with a ø particle size> 1 mm and a fraction with a particle ø of <1 mm. The physical properties of the biosorbent are shown in Table 1 and were determined following the methodology described in our previous work (Vera *et al*., 2016).

Table 1. Physical Properties of the cocoa shell.

Property	**Value**
Particle density (ρ_p)	1.127 g/ml
Particle porosity (ε)	0.4312
Point of zero charges (pH_{pzc})	6.96
Bed void fraction (ε_L)	0.6806

Cadmium nitrate and lead nitrate acquired as certified standards of 1 000 ppm traceable to NIST were used to prepare two synthetic solutions with a concentration of 10 mg / L of Cd2+ and Pb^{2+} each, using distilled water for the corresponding dilutions. The pH of the metallic solutions was

adjusted to 5 by adding 0.1 N HCl because the metals are found as cations at this pH, according to Bermejo (2016). All chemical agents used in this study were Merck brand analytical grade.

The removal tests were carried out in a glass column, whose dimensions are: diameter and height of 1.6 cm and 50 cm, respectively. The operating conditions were: particle size of the biosorbent>1 mm (coarse fraction), bed height of 10.5 cm, 7 g of biomass for the filling, and a feed flow rate of 1.9 ml/min. These conditions result from a previous hydrodynamic column study (Vera *et al*., 2018).

The experimental assembly of the column was carried out as described below. At the bottom of the column, gravel with a φ of 2 mm was placed so that the biosorbent particles were not entrained; the biosorbent was packed in the interior of the columns up to the bed height corresponding to each experiment. Subsequently, it was filled with gravel of a φ of 5 mm in the column's upper part to avoid the bed's floating and the loss of material. The system operation was carried out with a downward flow; the experiments were carried out at 18 °C. Before passing the metal solution through the biosorption column, the material was moistened with 300 ml of deionized water to avoid a sudden decrease in the metal concentration in the outlet solution. During the process, samples were collected at the outlet of the column, with an interval of 44 minutes for each sample, and a total of 20 samples were collected up to 836 minutes.

Tecnología y Ciencias del Agua

OPEN ACCESS

Check for updates

Quantification of metal concentration

The lead and cadmium concentrations of the synthetic solutions prepared and the samples collected at the outlet of the column were determined using the PERKIN ELMER AANALYST 400 atomic absorption technique.

Dynamic simulation in Aspen Adsorption® V10

Aspen Properties® provided the physical properties of these electrolytes in combination with water. The thermodynamic method used was ELECNRTL (Electrolyte Non-random Two-Liquid).

The ion exchange process was assumed as the main adsorption mechanism for metals. The assumptions made for the bed model were:

a) An upwind Differencing Scheme (USD1) was chosen as the discretization method with 20 nodes.

b) The mass balance was performed for the liquid phase assuming convection with estimated dispersion.

c) The superficial velocity of the fluid through the bed is constant, and its pressure loss is calculated with the Carman-Kozeny equation.

d) Lumped Resistance in linear function was chosen as the kinetic model and is a function of the solid.

e) The mass transfer coefficients (kc) for Cd2 + and Pb2 + are considered constant throughout the entire bed; however, they depend on the feed flow rate.

f) The Langmuir isotherm was assumed as an equilibrium model, and its parameters were obtained from previous studies (He *et al*., 2017; Li *et al*., 2016; Mohamed *et al*., 2016).

g) The isothermal and adiabatic system was considered for energy balance.

Validation and simulation parameters

To validate the breakthrough curve obtained with the simulator, the simulation was performed for Cd2+ and Pb^{2+} under the same experimental conditions (flow rate of 1.9 ml/min, the initial metal concentration of 10 mg/L, bed height of 10.5 cm, bed diameter of 1.6 cm, particle size >1 mm, and temperature of 18 °C). The breakthrough and saturation times were compared, referencing the current legislation in

Ecuador. Two error functions (SSE and X^2) and the coefficient of determination (R^2) were analyzed. After validation with the simulator, breakthrough curves were obtained varying the bed height: 7.5 cm, 9, 10.5, and 12 cm, while the concentration and flow were kept constant. Similarly, to determine the flow rate's effect, it varied between 1.1, 1.5, 1.9, and 2.3 ml/min while the other parameters were kept constant. The specified range of parameters was chosen because they are the most common in experimental adsorption studies carried out in a glass burette in a laboratory (Chen *et al*., 2019; Mohamed *et al*., 2016).

To meet the simulator requirements, parameters such as the total cation exchange capacity of the biosorbent (Q) and the mass transfer coefficients (k_c) were calculated using Eqs. (1) and (2). Since kc is a function of the velocity through the bed, this was calculated for each flow rate and is summarized in Table 2.

$$Q = \rho_r q_m (1 - \varepsilon_L) \tag{1}$$

$$\frac{k_c D_p}{D_{AB}} = 2 + 1.1 \left(\frac{D_p u \rho}{\mu}\right)^{0.6} \left(\frac{\mu}{\rho D_{AB}}\right)^{\frac{1}{3}} \tag{2}$$

Table 2. Mass transfer coefficients at different flow rates.

Flow rate (ml/min)	Mass transfer coefficient k_c (10^{-6} m/s)	
	Cd^{+2}	Pb^{+2}
1.1	5.412	6.102
1.5	6.016	6.769
1.9	6.559	7.367
2.3	7.057	7.916

In equations (1) and (2), ρ_r is the bulk density (g/m^3); q_m is the maximum adsorption capacity of the adsorbent on each metal (eq/g); this was obtained from preliminary studies (Bermejo, 2016; Sánchez-Salamea, 2016); ε_L is the bed porosity; D_p is the average particle diameter (m); u is the superficial velocity (m/s); ρ and μ are the density (kg/m^3) and Dynamic viscosity of the metal solution (kg/m.s), and D_{AB} is the diffusivity of the cation in the solution (m^2/s). For the specific case of the corresponding electrolytes of the salts of $Cd(NO_3)_2$ and $Pb(NO_3)_2$ that are formed when preparing the solution, the D_{AB} was calculated using Equation (3):

$$D_{AB} = \frac{n_{catión} + n_{anión}}{\frac{n_{anión}}{D_{catión}} + \frac{n_{catión}}{D_{anión}}} \quad (3)$$

Where n is the valence of the ion and D is the individual diffusivity of each ion. The diffusivity of the three ions (Pb^{2+}, Cd2+, and NO3-) was obtained from the literature.

Error analysis

To evaluate the fit of the simulator breakthrough curve to the experimental breakthrough curve data, two different error functions were examined (He *et al*., 2017; Li *et al*., 2016; Mohamed *et al*., 2016), which are described below.

Sum of squared error (SSE):

$$SSE = \sum_{i=1}^{n}(x_{i,cal} - x_{i,meas})^2 \quad (4)$$

Chi-Squared error (X^2):

$$X^2 = \sum_{i=1}^{n} \frac{(x_{i,cal} - x_{i,meas})^2}{x_{i,cal}} \quad (5)$$

Where $x_{i,meas}$ are the experimental C/C0 values and $x_{(i,\ cal)}$ corresponds to the C/C_0 values obtained from the simulator, and n represents the total number of data or C/C_0 values. Finally, the two breakthrough curves (experimental and simulator) were compared using the coefficient of determination (R^2):

$$R^2 = 1 - \frac{\sum_{i=1}^{n}(x_{i,cal} - x_{i,meas})^2}{\sum_{i=1}^{n}(x_{i,meas} - \bar{x})^2} \quad (6)$$

Where $\bar{x}$ Is the average of the experimental C/C0 values.

Results and discussion

Experimental studies

Figure 1a shows the breakthrough curves (C/C0 vs. time) for Cd2+ and Pb^{2+} obtained from the experimental tests carried out in a fixed-bed

column packed with cocoa shells at the established conditions. In the same way, Fig. 1b displays the curve of adsorbed metal (Cads) *versus* time.

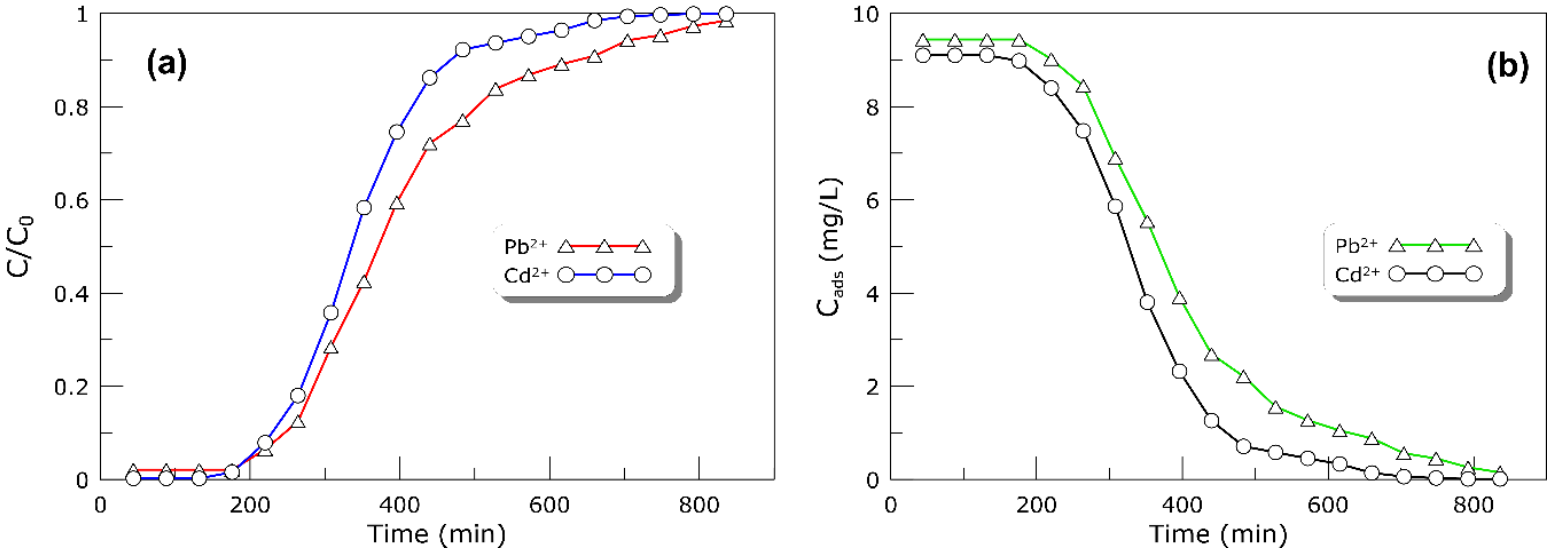

Figure 1. The experimental breakthrough curve for the adsorption of Cd2+ and Pb^{2+} in a fixed-bed column packed with cocoa shell.

From experimental curve Cads *vs*. time for both metals, It is observed that the area under the curve is greater for Pb^{2+} than for Cd2+, deducing that the active sites of the cocoa shell have a greater affinity for Pb^{2+} than for Cd2+, which leads to greater removal of this metal and a higher adsorption capacity—taking as a criterion, the maximum permissible limits allowed in Ecuador for Cd2+ and Pb^{2+} in wastewaters of 0.02 and 0.2 mg/L respectively. The curves show that the breakthrough

times for Cd2+ and Pb^{2+} do not differ significantly (129 and 171 min, respectively). In contrast, the saturation times (95 % initial concentration) for both metals vary by approximately 165 minutes. The greater affinity that the cocoa shell has for Pb^{2+} than for Cd2+ has already been reported in several studies. Lara, Tejada, Villabona, Arrieta, and Granados-Conde (2017) reported removal percentages of 91.32 % and 87.80 % for Pb^{2+} and Cd2+, respectively, while Meunier, Laroulandie, Blais, and Tyagi (2003) shows the preferential elimination of cocoa shells by Pb^{2+} with 94 %, followed by Cr3+ and Cd2+ (82 %). The justification for this event may be due to the ionic radius of the cations present or to the difference in electronegativity between Pb^{2+} and Cd2+.

The high electronegativity of the Pb^{2+} ion compared to Cd2+ (1.9> 1.69) might be the most likely factor that provides a stronger attraction with the adsorbent. In addition to Table 2, it is shown that the mass transfer coefficient for the experimentation flow rate (1.9 ml/min) is slightly higher for Pb^{2+}, which implies a higher adsorption rate for Pb^{2+}.

Validation with Aspen Adsorption®

Tecnología y Ciencias del Agua

OPEN ACCESS

Check for updates

To determine the effectiveness of the Aspen Adsorption® software in predicting the dynamic behavior of the biosorption process, the simulation of the biosorption of Cd2+ and Pb^{2+} with cocoa shells was carried out under the same experimental conditions. Figure 2 shows the simulated and experimental breakthrough curves for both metals.

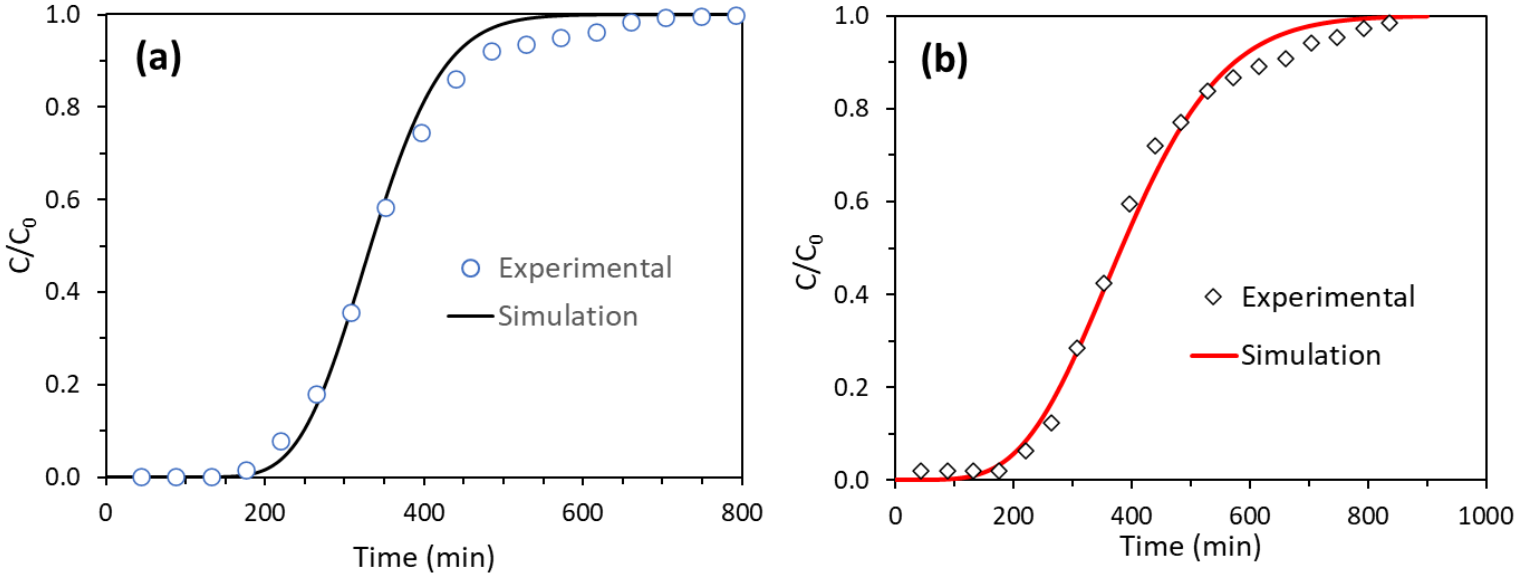

Figure 2. Simulated and experimental breakthrough curves for Cd2+ (a) and Pb^{2+} (b) with a flow rate of 1.9 ml/min, a metal concentration of 10 mg/L, and a bed height of 10.5 cm.

As can be seen, the simulated and experimental breakthrough curves have the same sigmoid shape, and both curves coincide in the trajectory of the initial and transitional region; In contrast, the final region

of both curves is slightly different; the difference is more pronounced in the case of Pb^{2+}. Similar behavior was found by Zhang, Adi, Huang, and Lin (2019) when simulating the adsorption of Cr3+ and Cu2+ on biochar in Aspen Adsorption, as in this study, the experimental and simulated breakthrough curves only differ in the final region. Because the curves are very similar in the initial region, the values of the breakthrough time in both curves are practically the same for both metals (Table 3). In contrast, the difference between the values of the saturation time differs markedly, in 72 min for Cd2+ and 171 min for the case of Pb^{2+}. Despite this, the high value of the coefficient of determination (R^2> 0.95) with comparatively lower values of SSE (< 0.05) and X^2 (<75) confirm that the results obtained with the simulation are ideally adjusted to the experimental data for both metals. However, the adjustment is more favorable for the case of Cd2+ than for $Pb^{2+,}$ according to R^2 (0.9984 > 0.9846). In the literature, other studies have validated the effectiveness of the Aspen Adsorption model to simulate the breakthrough curve, such as the studies by Juela (2020) on the adsorption of acetaminophen and Ahmed *et al*. (2020) on the melanoidin removal with fly ash. However, in almost all the breakdown curves predicted by the model, the similarity is more accurate in the initial region, and they differ in the final region, as obtained in the present study.

Table 3. Experimental and simulation results.

Parameter		Pb^{+2}	Cd^{+2}
Breakthrough time (min)	Experimental	171	129
	Simulation	172	127
Saturation time (min)	Experimental	735	572
	Simulation	564	500
SSE		0.0431	0.0051
X^2		70.2627	2.0043
R^2		0.9846	0.9984

Effect of bed height

Figure 3 (a and b) illustrate the influence of bed height on the breakthrough curves obtained for the biosorption of Cd2+ and Pb^{2+}. In comparison, Table 4 presents the breakthrough and saturation times obtained from curves 3a and 3b at different bed heights.

Tecnología y Ciencias del Agua

OPEN ACCESS

Check for updates

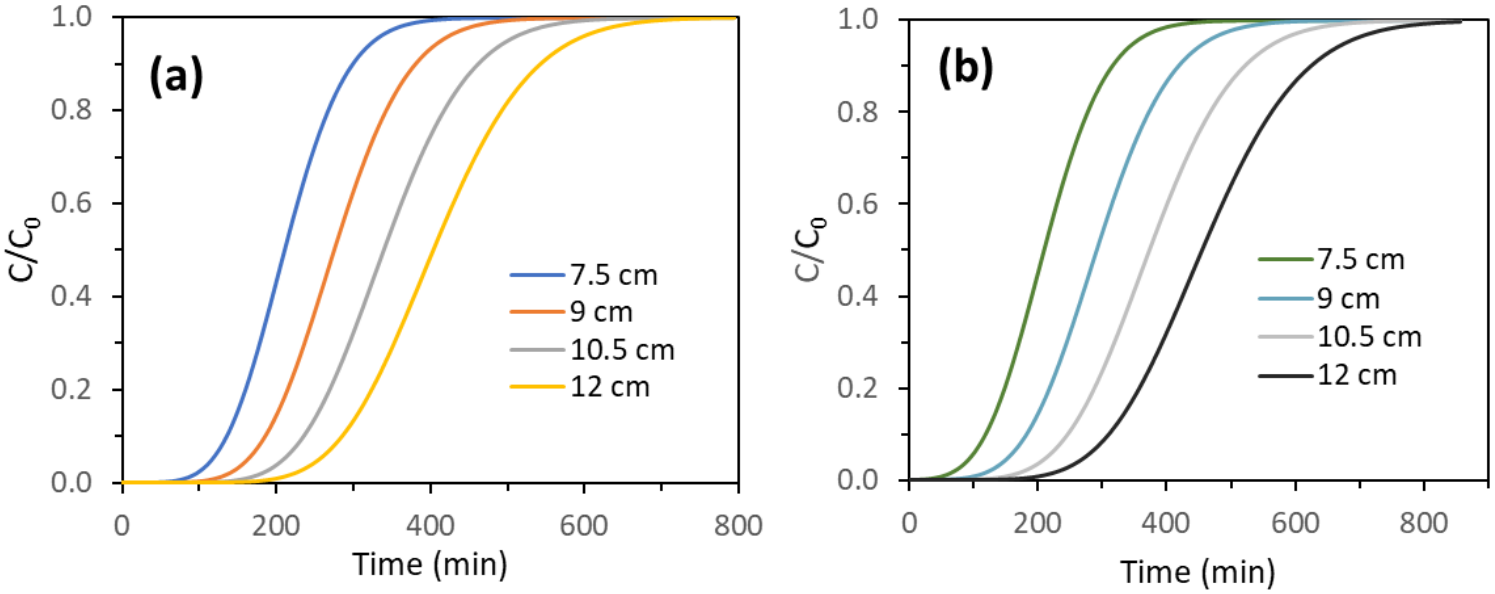

Figure 3. Breakthrough curves for Cd2+ (a) and Pb^{2+} (b) varying the bed height, with a flow rate of 1.9 ml/min and a metal concentration of 10 mg/l.

Table 4 shows the breakthrough and saturation time increase as the bed height increases. The breakthrough time increases from 60.34 min to 160.91 min for Cd2+ and from 148.15 min to 357.15 min for Pb^{2+} as the bed height increases from 7.5 cm to 12 cm. The same happens for the saturation time. By increasing the height of the bed, there is greater mass and surface area, increasing the active sites available for the adsorption of metals, which leads to longer breakthrough times. Besides, by increasing the height of the bed, the contact time between the metal and

the active sites of the biomass will increase. Consequently, the bed will take longer to saturate (Ahmad & Hameed, 2010).

Table 4. Breakthrough and saturation time for Cd2+ and Pb^{2+} varying the bed height.

Bed height (cm)	Breakthrough time (min)		Saturation time (min)	
	Cd^{+2}	Pb^{+2}	Cd^{+2}	Pb^{+2}
7.5	60.34	148.15	326.86	343.92
9	90.51	216.94	412.34	455.04
10.5	125.71	288.36	499.84	566.15
12	160.91	357.15	586.33	671.97

The effect of bed height variation on the breakdown curve may also be due to flow behavior inside the column. At low bed heights, the effects of axial dispersion can be considerable and predominant in mass transfer phenomena, leading to a difficult and slow diffusion of metal ions from the liquid phase to the solid phase, as Lin *et al*. (2017). Something important that is observed is that at all the heights studied, both the breakthrough and saturation time are always greater in the case of Pb^{2+} than for Cd2+, which confirms the preferential adsorption of the cocoa shell by Pb^{2+}.

Tecnología y Ciencias del Agua

OPEN ACCESS

Check for updates

Effect of flow rate

The effect of the flow rate through the column was studied at flows of 1.1, 1.5, 1.9, and 2.3 ml/min while keeping the bed height constant at 10.5 cm and an initial concentration of 10 mg/L of each metal.

Figure 4 (a and b) show the results of the simulated breakthrough curves at different flow rates.

Tecnología y Ciencias del Agua

OPEN ACCESS

Check for updates

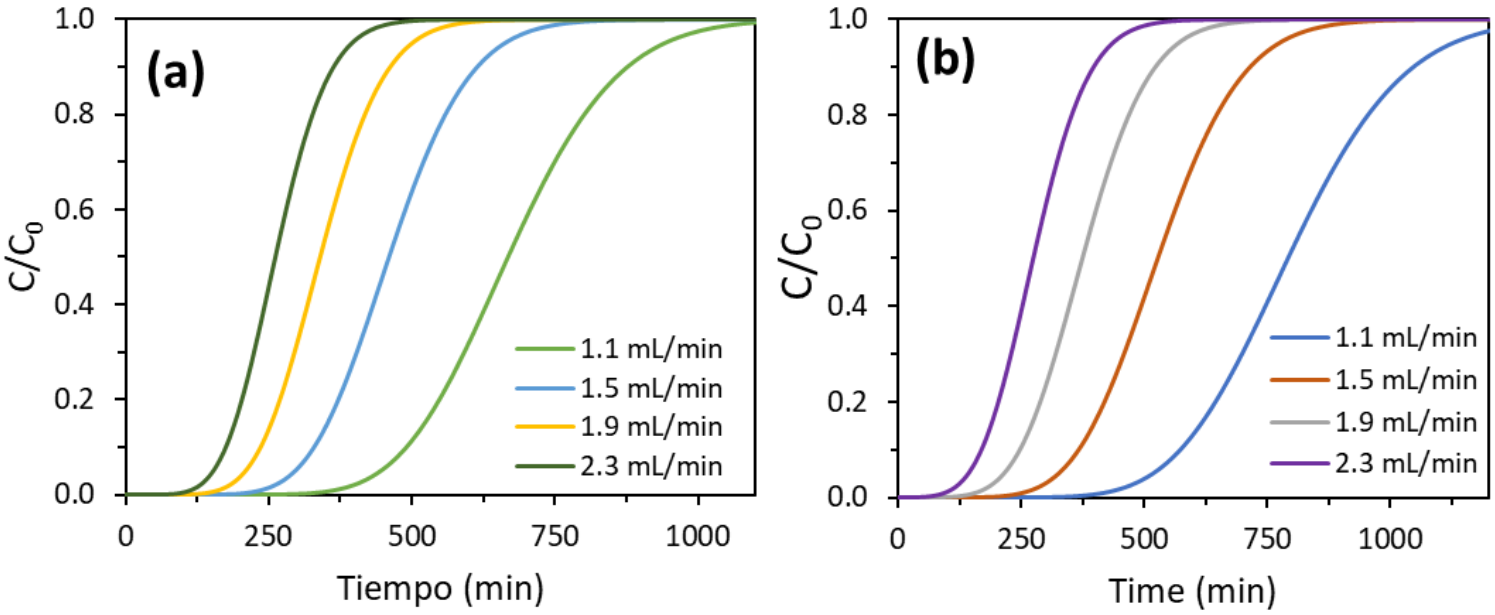

Figure 4. Breakthrough curves for Cd2+ (a) and Pb^{2+} (b) varying the flow rate, with a bed height of 10.5 cm and a metal concentration of 10 mg/l.

As the flow rate decreases, the breakthrough and saturation times increase. Table 5 shows the results, confirming that when the flow rate is low, the contact time and residence time in the bed will be greater, which translates into more effective adsorption of metals. At the same time, high flow rates tend to drive turbulence within the interstitial spaces of the bed, increasing the possibility that axial dispersion effects will occur and limiting metal diffusion into the pores of the adsorbent. Furthermore, at higher flow rates, the time the metal solution is in contact with the adsorbent is shorter. As a result, the adsorbate solution leaves the column

faster without reaching equilibrium, and the adsorption of metals is low. A similar effect was observed in the simulation of Cd2+ and Cu2+ with low saturation and breakthrough times at the highest feed flow rate (Soriano, Orfiana, Pangon, Nieva, & Adornado, 2016).

Table 5. Breakthrough and saturation time for Cd2+ and Pb^{2+} vary the flow rate.

Flow rate (ml/min)	Breakthrough time (min)		Saturation time (min)	
	Cd^{+2}	Pb^{+2}	Cd^{+2}	Pb^{+2}
1.1	301.71	645.52	940.34	1116.43
1.5	191.09	418.00	661.25	767.22
1.9	125.71	288.36	499.84	566.15
2.3	85.49	201.06	394.74	433.87

In addition, the higher the feed flow rate, the curve becomes much steeper and steeper, resulting in a smaller mass transfer zone as the flow increases. Consequently, the adsorption capacity decreases, and the adsorbent becomes saturated in a short operation time. Additionally, it is known that the adsorption kinetics of the metal in the adsorbent is directly proportional to the mass transfer coefficient (kc); consequently, if the flow rate increases, kc also increases (Table 2), which causes the rate of

adsorption of the metal on the cocoa shell to be faster, and the breakthrough and saturation times are reduced (Mohammed *et al*., 2013; Taseidifar *et al*., 2017).

Figure 5a shows the bed height's breakthrough time (tb) and saturation time (ts). The graph shows an increasing linear dependence of tb and ts with the bed height for both metals, with correlation coefficients (R^2) greater than 0.9. This way, it is established that tb and ts are directly proportional to the bed height when the flow rate and initial concentration are kept constant. Similar linear dependence of the breakthrough and saturation time with the bed height was observed in the furfural adsorption in fly ash (Singh, Srivastava, Goyal, & Mall, 2019).

The dependence of breakthrough and saturation time concerning the feed flow rate is a potential function with a negative exponent (Figure 5b); thus, tb and ts tend to decrease with increasing flow rates. From the behavior and shape of these curves, it could be predicted that, at sufficiently high flow rates, the breakthrough and saturation time could be kept constant; this effect could be advantageous since it would allow treating high volumes of effluents with the same amount of biomass. However, it should be mentioned that this increase could be favorable only up to a limited flow rate value; beyond this limit, it could cause flooding problems in the bed.

Tecnología y Ciencias del Agua

OPEN ACCESS

Check for updates

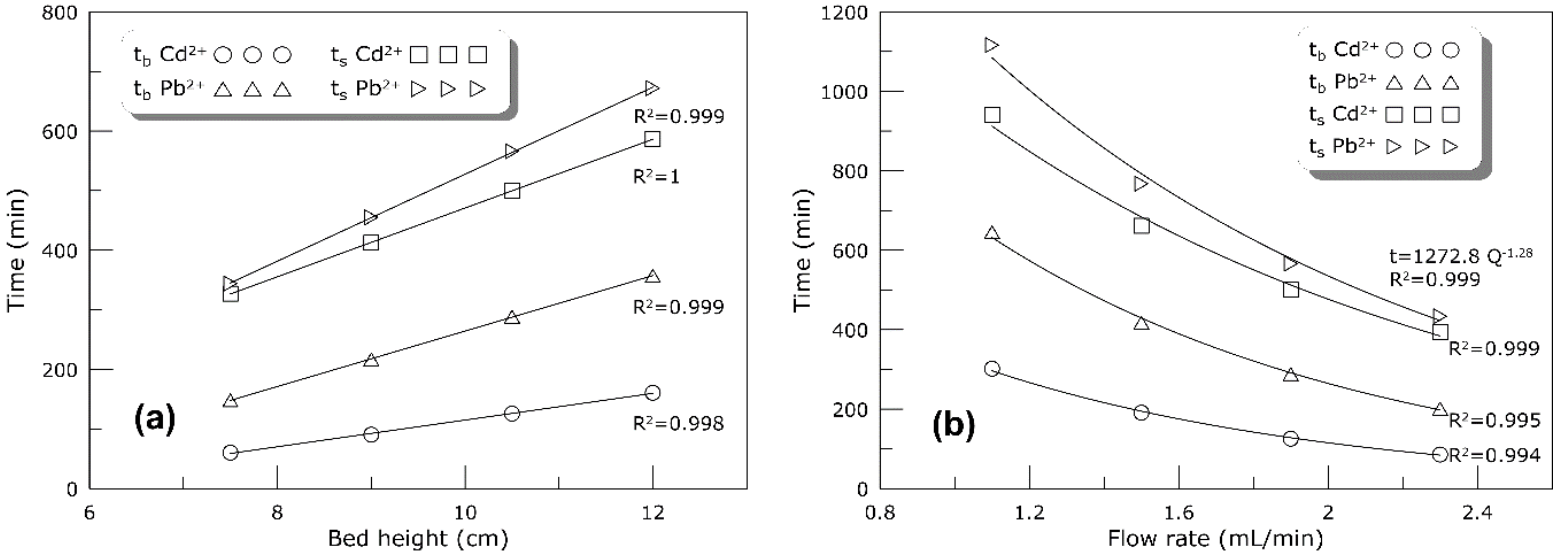

Figure 5. Effect of bed height (a) and feed flow rate (b) on breakthrough and saturation time.

Study of metal concentration through the fixed bed

The saturation of the column with time can be seen in Figure 6 (a and b) for Pb^{2+} and Cd2+, respectively. These graphs show the concentration of Pb^{2+} and Cd2+ in the liquid phase that is inside the column at different times of operation of the column; the saturated bed length (C = C0 = 10 mg/l), the mass transfer zone, and the fresh bed length can also be

observed (C = 0 mg/L). It can be seen that, at 200 minutes of operation, the saturated bed length is roughly 1 cm and 2.5 cm when the solution of Pb^{2+} and Cd2+ is passed, respectively. Similarly, after 500 minutes of operation, the saturated bed length is 5 cm for Pb^{2+} but approximately 9 cm for the case of Cd2+; hence the column is saturated in less time when the Cd2+ solution is passed through. Something that can also be highlighted in Figure 6 (a and b) is the notable difference in the length of the mass transfer zone (MTZ) between both metals. In the case of Pb^{2+} adsorption, the ZTM is approximately 8.5 cm long at 100 min, while for Cd2+, the MTZ is only 6.5 cm simultaneously. For that reason, a reduced mass transfer zone means lower adsorption capacity and shorter saturation times. Similar results were obtained by Lin *et al*. (2017) on levulinic acid adsorption.

Tecnología y Ciencias del Agua

OPEN ACCESS

Check for updates

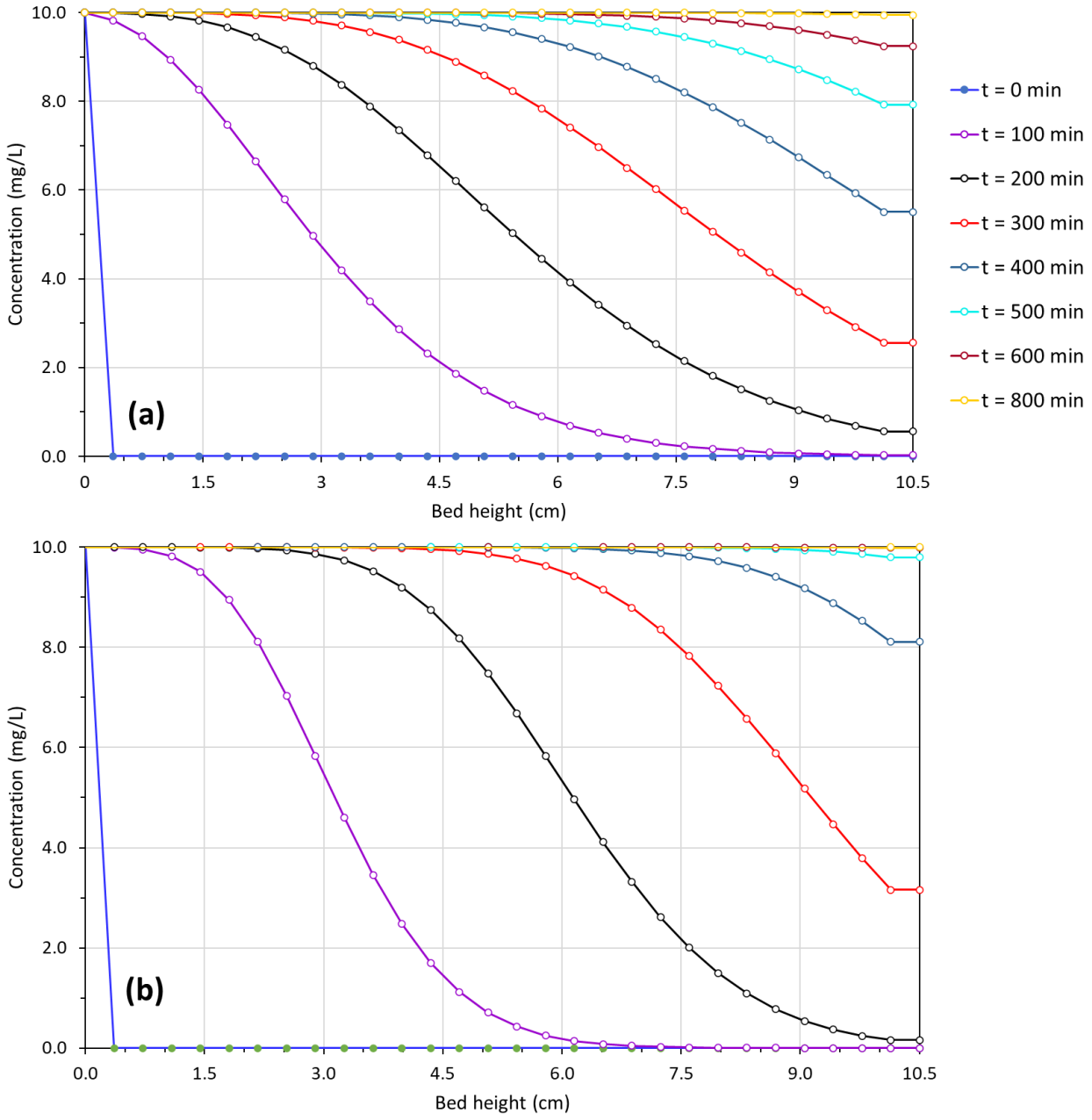

Figure 6. Variation of the Pb^{2+} (a) and Cd2+ (b) concentration through the bed.

Tecnología y Ciencias del Agua

OPEN ACCESS

Check for updates

Conclusions

The active sites of the cocoa shell have a higher affinity for the lead cation than for cadmium; the high electronegativity of the Pb^{2+} ion may be the most probable factor that explains the preferential adsorption of the cocoa shell on this metal. The experimental data allowed to validate of the results obtained with the Aspen Adsorption simulator; the simulated breakthrough curve converges with the experimental curve in almost the entire trajectory, a coefficient of determination (R^2) close to unity was obtained, and the value of the error (SSE) was negligible. The effect produced by the bed height and flow rate in breakthrough and saturation time could be predicted with a good approximation using the software, verifying that by increasing the bed height and decreasing the flow rate, a higher breakthrough and saturation time is obtained. It was also observed that lead adsorption had a larger mass transfer zone than cadmium adsorption. The results of this study expose the use of Aspen Adsorption as a potential and effective alternative to simulate the dynamic behavior of heavy metal biosorption processes in fixed-bed columns.

Tecnología y Ciencias del Agua

OPEN ACCESS

Check for updates

Acknowledges

The authors thank the Center for Environmental Studies of the University of Cuenca for the support provided in carrying out all the experiments.

References

Ahmad, A. A., & Hameed, B. H. (2010). Fixed-bed adsorption of reactive azo dye onto granular activated carbon prepared from waste. *Journal of Hazardous Materials*, 175(1-3), 298-303. Recovered from https://doi.org/10.1016/j.jhazmat.2009.10.003

Ahmed, S., Unar, I. N., Khan, H. A., Maitlo, G., Mahar, R. B., Jatoi, A. S., Memon, A. Q., & Shah, A. K. (2020). Experimental study and dynamic simulation of melanoidin adsorption from distillery effluent. *Environmental Science and Pollution Research*, 27(9), 9619-9636. Recovered from https://doi.org/10.1007/s11356-019-07441-8

Akif, M., Khan, A. R., Hussain, Z., Maal-Abrar, Khan, M., Sok, K., Min, Z., & Muhammad, A. (2002). Textile effluents and their contribution towards aquatic pollution in the Kabul River (Pakistan). *Journal of the Chemical Society of Pakistan*, 24(2), 106-111. Recovered from https://inis.iaea.org/search/search.aspx?orig_q=RN:33069917

Akpor, O., Ohiobor, B., & Olaolu, T. (2014). Heavy Metal Pollutants in Wastewater Effluents: Sources, Effects and Remediation. *Advances in Bioscience and Bioengineering*, 2(4), 37-43.

Bermejo, D. F. (2016). *Remoción de plomo y cadmio presente en aguas residuales mineras mediante biosorción en columnas con bagazo de caña y cáscara de cacao*. Recovered from http://dspace.ucuenca.edu.ec/jspui/bitstream/123456789/25710/1/Tesis.pdf

Besante, J., Niforatos, J., & Mousavi, A. (2011). Cadmium in rice: Disease and social considerations. *Environmental Forensics*, 12(2), 121-123.

Byambaa, M., Dolgor, E., Shiomori, K., & Suzuki, Y. (2018). Removal and recovery of heavy metals from industrial wastewater by precipitation and foam separation using lime and casein. *Journal of Environmental Science and Technology*, 11(1), 1-9. Recovered from https://doi.org/10.3923/jest.2018.1.9

Cegłowski, M., & Schroeder, G. (2015). Preparation of porous resin with Schiff base chelating groups for removal of heavy metal ions from aqueous solutions. *Chemical Engineering Journal*, 263, 402-411.

Chen, Z. L., Zhang, J. Q., Huang, L., Yuan, Z. H., Li, Z. J., & Liu, M. C. (2019). Removal of Cd and Pb with biochar made from dairy manure at low temperature. *Journal of Integrative Agriculture*, 18(1), 201-210. Recovered from https://doi.org/10.1016/S2095-3119(18)61987-2

Ferniza-García, F., Amaya-Chávez, A., Roa-Morales, G., & Barrera-Díaz, C. E. (2017). Removal of Pb, Cu, Cd, and Zn present in aqueous solution using coupled electrocoagulation-phytoremediation

treatment. *International Journal of Electrochemistry*, 2017, 1-11. Recovered from https://doi.org/10.1155/2017/7681451

Gherasim, C., & Mikulášek, P. (2014). Influence of operating variables on the removal of heavy metal ions from aqueous solutions by nanofiltration. *Desalination*, 343, 67-74.

Guo, L., Du, Y., Yi, Q., Li, D., Cao, L., & Du, D. (2015). Efficient removal of arsenic from "dirty acid" wastewater by using a novel immersed multi-start distributor for sulphide feeding. *Separation and Purification Technology*, 142, 209-214. Recovered from https://doi.org/10.1016/j.seppur.2014.12.029

He, J., Li, Y., Wang, C., Zhang, K., Lin, D., Kong, L., & Liu, J. (2017). Rapid adsorption of Pb, Cu and Cd from aqueous solutions by β-cyclodextrin polymers. *Applied Surface Science*, 426, 29-39. Recovered from https://doi.org/10.1016/J.APSUSC.2017.07.103

Jokar, M., Mirghaffari, N., Soleimani, M., & AJabbari, M. (2019). Preparation and characterization of novel bio ion exchanger from medicinal herb waste (chicory) for the removal of Pb2+ and Cd2+ from aqueous solutions. *Journal of Water Process Engineering*, 28, 88-99.

Juela, D. M. (2020). Comparison of the adsorption capacity of acetaminophen on sugarcane bagasse and corn cob by dynamic simulation. *Sustainable Environment Research*, 30(1), 23. Recovered from https://doi.org/10.1186/s42834-020-00063-7

Khan, Z., Ahmad, K., Ashraf, M., & Parveen, R. (2015). Bioaccumulation of heavy metals and metalloids in luffa (*Luffa cylindrica L.*). Irrigated with domestic wastewater in Jhang, Pakistan: A prospect for human nutrition. *Pakistan Journal of Botany*, 47(1), 217-224.

Khanipour, A., Ahmadi, M., & Seifzadeh, M. (2018). Study on bioaccumulation of heavy metals (cadmium, nickel, zinc and lead) in the muscle of wels catfish (*Silurus glanis*) in the Anzali Wetland, Iran. *Journal of Fisheries Science*, 17(1), 244-250.

Khosa, M. K., Jamal, M. A., Hussain, A., Muneer, M., Zia, K. M., & Hafeez, S. (2013). Efficiency of aluminum and iron electrodes for the removal of heavy metals [(Ni (II), Pb (II), Cd (II)] by electrocoagulation method. *Journal of the Korean Chemical Society*, 57(3), 316-321. Recovered from https://doi.org/10.5012/jkcs.2013.57.3.316

Kończyk, J., Żarska, S., & Ciesielski, W. (2019). Adsorptive removal of Pb(II) ions from aqueous solutions by multi-walled carbon nanotubes functionalised by selenophosphoryl groups: Kinetic, mechanism, and thermodynamic studies. *Colloids and Surfaces A: Physicochemical and Engineering Aspects*, 575, 271-282.

Kong, X., Ting, L., Ziheng, Y., Zhe, Ch., Da, L., Zhiwei, W., Hua, Z., Qiuhua, L., & Shanshan, Z. (2018). Heavy metal bioaccumulation in rice from a high geological background area in Guizhou Province, China. *International Journal of Environmental Research and Public Health*, 15(10), 2281.

Lara, C., Tejada, C., Villabona, A., Arrieta, A., & Granados-Conde, C. (2017). Adsorción de plomo y cadmio en sistema continuo de lecho fijo sobre residuos de cacao. *Revista ION: Investigación, Optimización y Nuevos Procesos en Ingeniería*, 29(2), 111-122.

Li, M., Zhang, Z., Li, R., Wang, J. J., & Ali, A. (2016). Removal of Pb(II) and Cd(II) ions from aqueous solution by thiosemicarbazone modified chitosan. *International Journal of Biological Macromolecules*, 86, 876-884. Recovered from https://doi.org/10.1016/J.IJBIOMAC.2016.02.027

Lin, X., Huang, Q., Qi, G., Shi, S., Xiong, L., Huang, C., Chen, X., Li, H., & Chen, X. (2017). Estimation of fixed-bed column parameters and mathematical modeling of breakthrough behaviors for adsorption of levulinic acid from aqueous solution using SY-01 resin. *Separation and Purification Technology*, 174, 222-231. Recovered from https://doi.org/10.1016/j.seppur.2016.10.016

Meunier, N., Laroulandie, J., Blais, F., & Tyagi, R. (2003). Cocoa shells for heavy metal removal from acidic solutions. *Bioresource Technology*, 90(3), 255-263.

Mohamed, E.-S. R., Ahmed, M. S., Tantawy, A. A., Gomaa, N. H., & Mahmoud, H. A. (2016). Phytoremediation of Pb+2, Cd+2 and Cu+2 by an aquatic macrophyte azolla pinnata from industrial wastewater in Egypt. *Middle East Journal of Applied Sciences*, 6(1), 27-39. Recovered from http://www.curresweb.com/mejas/mejas/2016/27-39.pdf

Mohammed, A. A., Ebrahim, S. E., & Alwared, A. I. (2013). Flotation and sorptive-flotation methods for removal of lead ions from wastewater using SDS as surfactant and barley husk as biosorbent. *Journal of Chemistry*, 2013, 1-6. Recovered from https://doi.org/10.1155/2013/413948

Musilova, J., Arvay, J., Vollmannova, A., Toth, T., & Tomas, J. (2016). Environmental contamination by heavy metals in region with previous mining activity. *Bulletin of Environmental Contamination and Toxicology*, 97(4), 569-575.

Rana, M., Tangpong, J., & Rahman, M. (2018). Toxicodynamics of lead, cadmium, mercury and arsenic. Induced kidney toxicity and treatment strategy: A mini review. *Toxicology Reports*, 5, 704-713.

Sánchez-Salamea, N. A. (2016). *Biosorción en tanque agitado de Cd+2 y Pb+2 con cáscara de cacao*. Recovered from https://dspace.ucuenca.edu.ec/bitstream/123456789/25242/3/Tesis.pdf

Schwarze, M., Groß, M., Moritz, G., Buchner, L., Kapitzki, L., Chiappisi, M., & Gradzielski, M. (2015). Micellar enhanced ultrafiltration (MEUF) of metal cations with oleylethoxycarboxylate. *Journal of Membrane Science*, 478, 140-147.

Singh, S., Srivastava, V. C., Goyal, A., & Mall, I. D. (2019). Breakthrough modeling of furfural sorption behavior in a bagasse fly ash packed bed. *Environmental Engineering Research*, 25(1), 104-113. Recovered from https://doi.org/10.4491/eer.2018.407

Soriano, A., Orfiana, O., Pangon, J., Nieva, A., & Adornado, A. (2016). Simulated biosorption of Cd(II) and Cu(II) in single and binary metal systems by water hyacinth (*Eichhornia crassipes*) using aspen Adsorption®. *ASEAN Journal of Chemical Engineering*, 16(2), 21-43.

Sörme, L., & Lagerkvist, R. (2002). Sources of heavy metals in urban wastewater in Stockholm. *Science of the Total Environment*, 298(1-3), 131-145.

Taseidifar, M., Makavipour, F., Pashley, R. M., & Mokhlesur-Rahman, A. F. M. (2017). Removal of heavy metal ions from water using ion flotation. *Environmental Technology and Innovation*, 8, 182-190. Recovered from https://doi.org/10.1016/j.eti.2017.07.002

Vera, L., García, N., Uguña, M., Flores, M., González, E., & Brazales, D. (2018). Modelado en columna de lecho fijo para la bioadsorción de cd+2 y pb+2 con cáscara de cacao. *Revista Internacional de Contaminación Ambiental*, 34(4), 611-620. DOI: 10.20937/RICA.2018.34.04.05

Vera, L., Uguña, M. F., García, N., Flores, M., Vázquez, V., & Aloma, I. (2016). Desarrollo de materiales sorbentes para la eliminación de metales pesados de las aguas residuales mineras. *Afinidad*. Recovered from https://www.raco.cat/index.php/afinidad/article/view/312048

Yadav, A., Yadav, K., & Shukla, D. (2013). Investigation of heavy metal status in soil and vegetables grown in urban area of Allahabad, Uttar

Pradesh, India. *International Journal of Scientific and Research Publication*, 3(9), 1-7.

Zhang, Y., Adi, V., Huang, H., & Lin, H. (2019). Adsorption of metal ions with biochars derived from biomass wastes in a fixed column: Adsorption isotherm and process simulation. *Journal of Industrial and Engineering Chemistry*, 76, 240-244.